Update on the NIST Second-Generation Room-Temperature Water Calorimeter

Heather Chen-Mayer and Ronald Tosh
Ionizing Radiation Division
National Institute of Standards and Technology
Gaithersburg, MD 20899 USA

April 10, 2009

This focused report summarizes certain experiments and theoretical work conducted at NIST over the past two years on the problem of heat transport in water calorimetry. In the course of this work, we have found that our approach of periodic exposure of the calorimeter to radiation (in order to achieve a steady-state condition for measurements of absorbed dose) is quite sensitive to details of heat transport between the external phantom and the interior of the glass vessel. Moreover, we find that to a significant degree such details can be controlled and, hence, isolated and studied carefully for purposes of developing appropriate corrective actions targeted for the calorimeter technologies with which we are working, viz. the original, thermistor-based design of Domen and the newer, high-precision ultrasonic calorimetry system.

We begin with a summary of recent data obtained from the thermistor-based calorimeter in ^{60}Co beams and simulations done with COMSOL Multiphysics, presented in Fig. 1. Each experimental data point was acquired over 20 hours (cumulative) of repeated exposure to a chopped beam in which the period was fixed at values ranging from 120 s to 1800 s. These data, plotted against the half period (or exposure time per cycle, t_open), show a pronounced variation of apparent dose rate, which, as we have discussed before, is a consequence of heat transport. The purpose of this run and several others we have done in both ^{60}Co and Clinac x-ray beams is to measure the effect very precisely, so that heat-transfer corrections could be specified to a precision approaching 0.1 %. The relative uncertainties of the experimental data vary from 0.1 % to 0.8 %, and so, in principle, this should be possible if most/all of the data in the plot could be used in a least-squares regression.

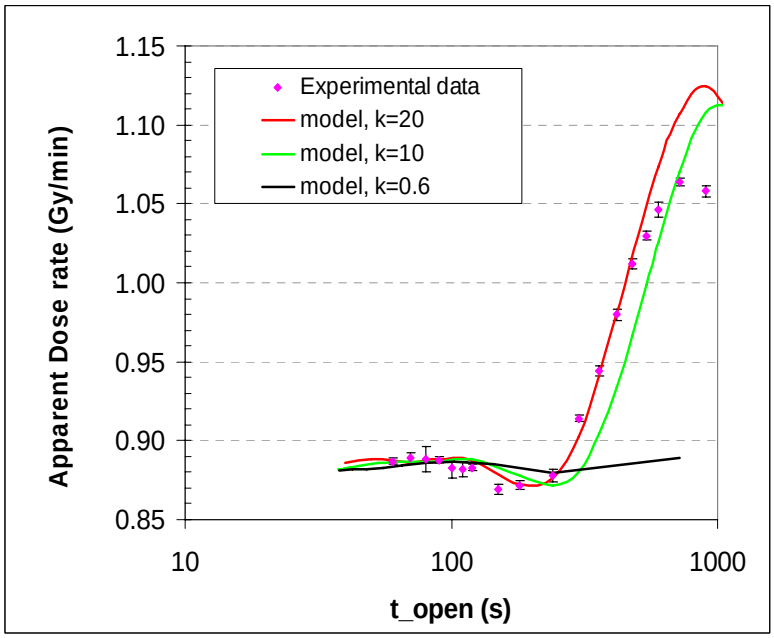

Figure 1. Measured dose rate as a function of shutter opening time, and the scaled output curves from model simulation.

For this purpose, we have performed chi-square minimization using finite-element simulations as the reference curve with a single parameter, an overall scaling factor, as the (unknown) dose rate. This assumed linear dependence of temperature rise on dose rate is a consequence of heat conduction, so that dose rate determines only the level of the asymptote at small t_open and the amplitude of the deviations from that asymptote at larger t_open. The shape of the curve in Fig. 1, *e.g.*, the location of extrema along the horizontal axis, is determined by the overlap of cell geometry with beam profile, the thermal diffusivity of the water inside the glass vessel, and the effective diffusivity of the water outside the glass vessel.

The use of an effective diffusivity – or, equivalently, effective thermal conductivity – for the water phantom (external to the vessel) is a simple approximation that is intended to account for the effect of continuous stirring of the phantom, which is done throughout the experimental run in order to redistribute heat in the external water as quickly as possible. The plots in Fig. 1 indicate how increasing this effective thermal conductivity, k, above that of static water (k = 0.6 W/mK) produces much better agreement between the simulation output and the experimental data. The use of stirring during irradiation might appear to introduce unnecessary complications into the experiment, and that turning it off would allow us to use a simpler model in our simulations. However, we have found that without stirring, large fluctuations arise in experimental measurements at the larger shutter periods, and that reproducibility is restored when the stirrer is turned back on. This suggests that natural convection in the external phantom, which we have observed to be an oscillatory phenomenon (and which would not exist when the stirrer is running), is perturbing the steady-state value of the temperature rise.

While stirring appears to reduce/eliminate errors due to natural convection in the exterior water, it might be expected to have much less of an effect on the development of natural convection within the vessel itself. At the present time, we are exploring the possibility that the deviation of the simulation output from the observed data at larger t_open in Fig. 1 might be a consequence of natural convection within the vessel. While we have better statistics at larger t_open, the systematic bias is greater, and vice versa for the region of smaller t_open. This has impeded our effort to obtain the desired ≈0.1 % precision in our heat-transport corrections, as it limits the number of usable data points as well as their precision in the chi-square procedure. If we are successful in augmenting the model, then it should be possible for us to back out the heat-transport effects in the data of Fig. 1 and identify the underlying dose rate.

The effort to quantify the effects of conduction and convection independently has led us to seek more convenient ways to produce them in our water calorimeters. For example, we have done some exploratory work with the Clinac, whose aperture, dose rate and chopping frequency are controlled electronically over much broader ranges than are achievable with our ^{60}Co treatment head. Another promising approach has been to utilize our precision water bath, normally used for calibrating our thermistor probes, as a source for controllable thermal stimuli that would enable us to study the thermal frequency response of the calorimeter vessel.

A schematic of the procedure used with the thermal bath for acquiring and analyzing data is shown in Fig. 2. Briefly, a stimulus consisting of a temperature square-wave is generated within the bath, and simultaneous measurements are made of the exterior temperature near the vessel and the interior temperature along the axis of the vessel. If allowed to run for enough cycles, such that transients in the thermal response decay sufficiently, the signals can be processed in the frequency domain, as shown in Fig. 2, to

generate a transfer function that is indicative of how the layer of water separating the two probes acts to attenuate and phase-shift the frequency components of the thermal stimulus.

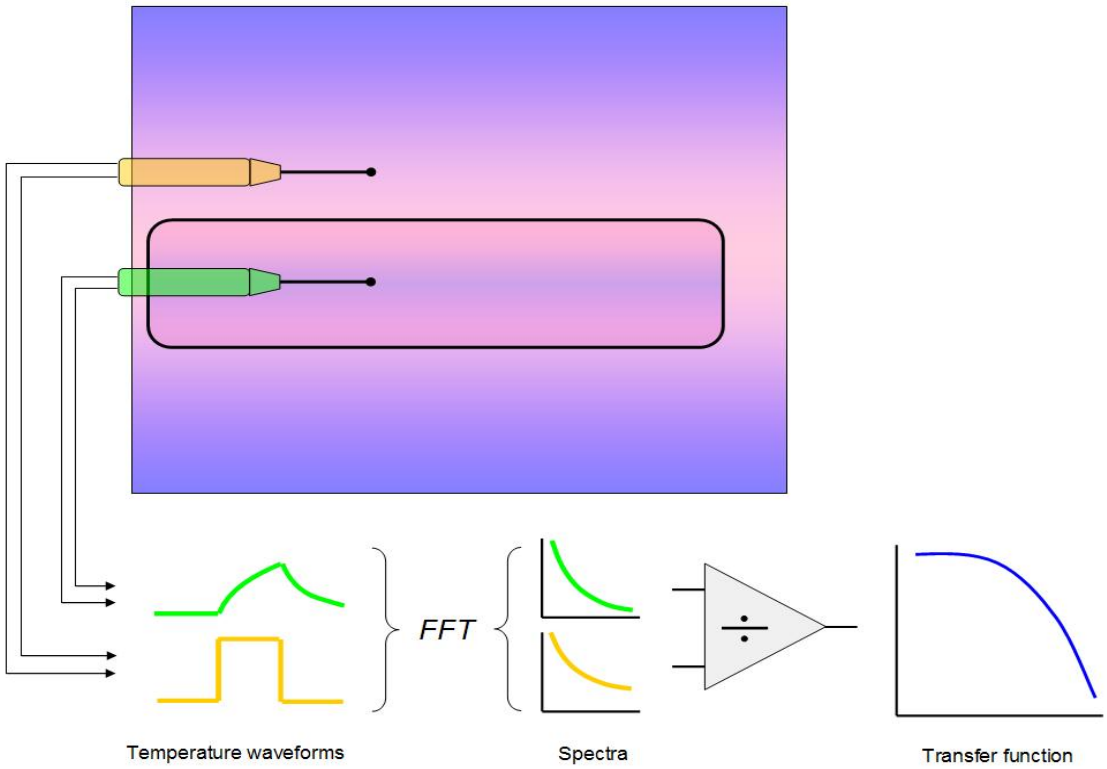

Figure 2. Schematic of experiments with the high-precision bath. Bath temperature is controlled by computer, and its value near the glass vessel is recorded by one thermistor probe (yellow) as a function of time. A second thermistor probe (green) simultaneously monitors internal temperature near the center of the glass vessel, and the two waveforms are processed in the frequency domain to obtain a transfer function that is characteristic of heat transport between the bath and the internal probe.

As noted above, the use of the bath for this type of measurement was originally conceived as a means by which to assess the thermal frequency response of the calorimeter vessel independent of the radiation beam (in addition to furnishing an automated thermistor-calibration procedure). The bath is ideally suited for this type of application because the timing characteristics and amplitude of the stimulus waveform can be designed to fit a wide variety of specifications; for example, heat transport would be expected to occur principally by conduction for small amplitude temperature stimuli centered at 4 ^{o}C, while natural convection would become more important with larger amplitude temperature oscillations about 4 ^{o}C and/or mean temperatures above 4 ^{o}C.

Results obtained for operation of the bath with a square-wave temperature profile with amplitude of 0.5 ^{o}C about a mean temperature of 4 ^{o}C are shown in Fig. 3. The plots show attenuation as a function of period (reciprocal of the frequency of the thermal stimulus), and show qualitatively what one expects: the internal temperature faithfully tracks the applied external temperature at longer periods, but suffers an increasing attenuation at shorter periods. The plots of measured data, computational simulation and analytical solution of the heat equation are in excellent agreement down to a period of about 150 s, where noise from truncation errors (due to finite resolution of the voltmeter) cause the curve to deviate upward from its expected monotonic decrease. The same artifact arises with the computational simulation, although its relatively higher numerical precision delays the onset until much

shorter periods. The analytical solution, of course, is not affected by this problem.

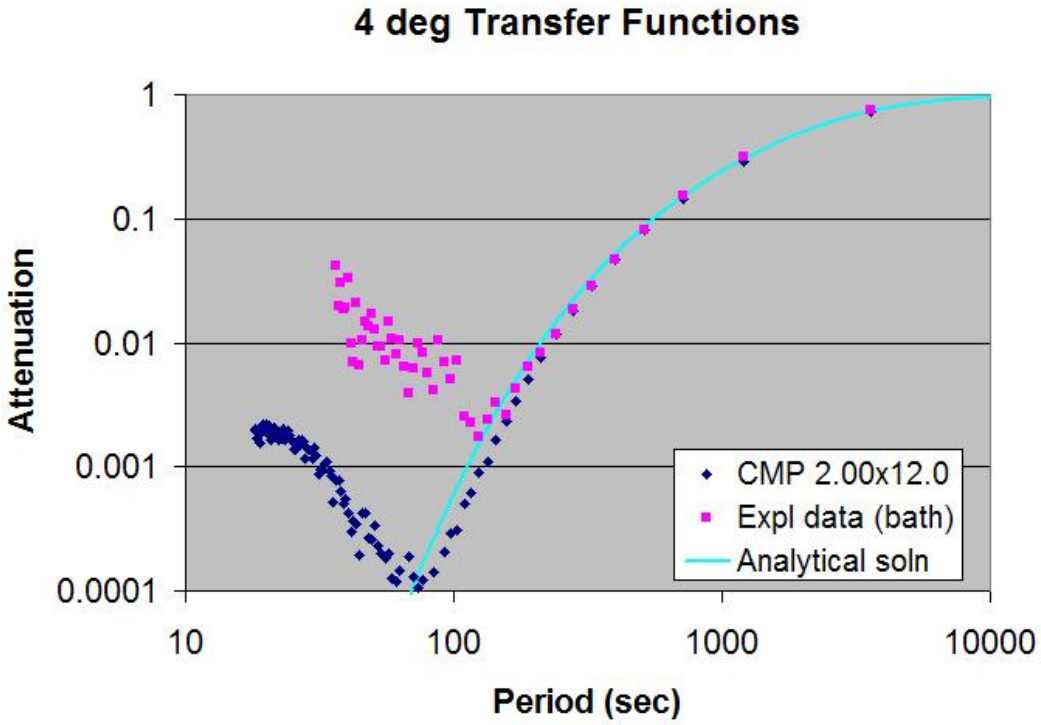

Figure 3. Transfer functions derived from the procedure shown in Fig. 1, plotted vs. period of the bath-temperature input waveform. The data shown in this plot were obtained under conditions in which the bath temperature was made to oscillate about 4 °C.

The attenuation shown in Fig. 3 is expected with heat conduction because the medium between the probes contains no heat sources. The same logic does not apply to natural convection, however, which builds up over time within the glass vessel if conditions are conducive. We have observed this effect as well, by restricting attention to even harmonics of the square-wave stimulus. A plot of that response is given in the larger NIST activities report, and shows high gain at mean bath temperatures above 4 °C and near-extinction in the vicinity of 4 °C, as might be expected based upon the known dependence of volume-expansion coefficient on temperature. Thus, we have at our disposal a means by which to isolate the effects of conduction and convection on the thermal frequency response of the vessel, and thereby obtain correction factors for heat transport that specifically take into account both effects in a way that can be validated outside the radiation beam.

This work might also yield useful insight into how convection and conduction work to distort temperature distributions within an open phantom, which is central to the operation of the ultrasonic thermometer we have been developing for dosimetry. Fig. 4 compares plots of experimental data derived from the cylindrical array described in the larger NIST activities report with output from COMSOL Multiphysics, under conditions in which an infrared beam derived from a heat lamp is turned on for 90 s. The data are estimates of temperature in a small volume at the center of the array, derived via a filtered back-projection algorithm. As seen in the figure, the temperature reaches an apparent saturation condition much more

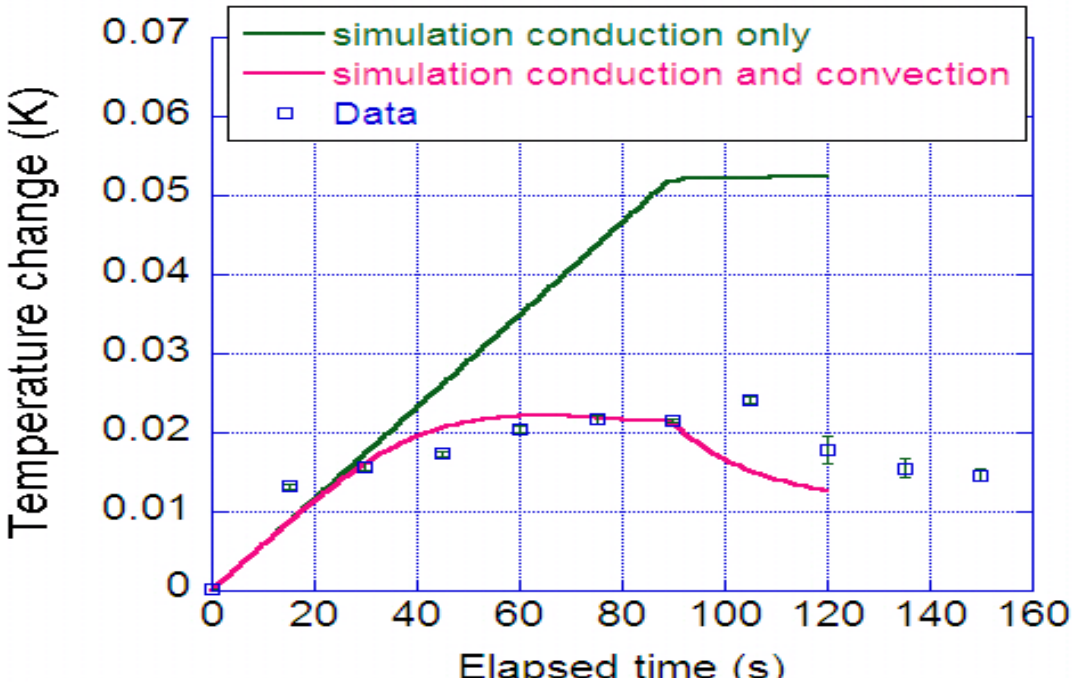

Figure 4. Temperature rise in water measured by an ultrasound tomographic system. Heat-transport simulations with conduction only (green) and both conduction and convection (red) suggest that convection in the open water is the principal heat-transport mechanism.

rapidly than can be explained by conduction alone; however, a much improved agreement results if convection is included in the simulation. Thus, with the ultrasonic instrument, we have the makings of a system that is capable of time-resolved, 2D temperature mapping that can record the rather complicated dynamics of buoyant convection in an open water phantom. When these effects are understood and can be deconvolved from the measured waveforms, extending this system to 3D with faster sampling might then yield an instrument that could be used to image absorbed-dose distributions from the types of beams used in modern radiotherapy.